SIAM J. APPL. MATH.
Vol. 73, No. 6, pp. 2004–2028

MODELING ARTERIAL WALL DRUG CONCENTRATIONS FOLLOWING THE INSERTION OF A DRUG-ELUTING STENT*

SEAN MCGINTY†, SEAN MCKEE‡, ROGER M. WADSWORTH§, AND CHRISTOPHER MCCORMICK¶

Abstract. A mathematical model of a drug-eluting stent is proposed. The model considers a polymer region, containing the drug initially, and a porous region, consisting of smooth muscle cells embedded in an extracellular matrix. An analytical solution is obtained for the drug concentration both in the target cells and the interstitial region of the tissue in terms of the drug release concentration at the interface between the polymer and the tissue. When the polymer region and the tissue region are considered as a coupled system, it can be shown, under certain assumptions, that the drug release concentration satisfies a Volterra integral equation which must be solved numerically in general. The drug concentrations, both in the cellular and extracellular regions, are then determined from the solution of this integral equation and used in deriving the mass of drug in the cells and extracellular space.

Key words. drug-eluting stent, atherosclerosis, Laplace transforms, branch points, analytical solution, Volterra integral equation

AMS subject classifications. 92C50, 35E99, 76R99, 76S99, 44A10

DOI. 10.1137/12089065X

1. Introduction.

Coronary heart disease (CHD) is the main cause of death in developed countries [32] and accounts for 18% of all deaths in the United States annually [27]. CHD is characterized by a blockage or occlusion of one or more of the arteries which supply blood to the heart muscle. This is due to atherosclerosis, a complex progressive inflammatory disease [25], which leads to the buildup of fatty plaque material near the inner surface of the arterial wall [29]. If left untreated, this leads to episodes of chest pain (angina). Ultimately, the atherosclerotic plaque is vulnerable to rupture, leading to the formation of a blood clot which blocks the artery, causing a heart attack. Until relatively recently, bypass surgery was required. However, in the majority of cases, this has now been replaced by inserting a small metallic cage, called a stent, into the occluded artery to maintain blood flow. When a stent is implanted into an artery, the endothelium is severely damaged. The consequent inflammatory response and excessive proliferation and migration of smooth muscle cells leads to the development of in-stent restenosis (ISR), a reocclusion of the artery which is a significant limitation of bare metal stents. The introduction of drug-eluting stents (DESs) significantly reduced the occurrence of ISR by releasing a drug to inhibit smooth muscle cell proliferation. However, their use has been associated

*Received by the editors September 7, 2012; accepted for publication (in revised form) August 16, 2013; published electronically November 12, 2013. This research was supported by EPSRC grant EP/J007242/1.
http://www.siam.org/journals/siap/73-6/89065.html
†Corresponding author. Department of Mathematics and Statistics, University of Strathclyde, Glasgow, G1 1XH, UK (s.mcginty@strath.ac.uk). This author's work was supported by a Carnegie Scholarship.
‡Department of Mathematics and Statistics, University of Strathclyde, Glasgow, G1 1XH, UK (s.mckee@strath.ac.uk).
§The author is deceased. Former address: Strathclyde Institute of Pharmacy and Biomedical Sciences, University of Strathclyde, Glasgow G4 0NR, UK.
¶Biomedical Engineering, University of Strathclyde, Glasgow G4 0NW, UK, and Strathclyde Institute of Pharmacy and Biomedical Sciences, University of Strathclyde, Glasgow G4 0NR, UK (christopher.mccormick@strath.ac.uk).

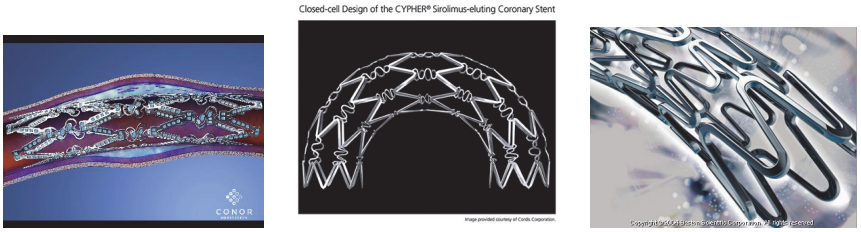

FIG. 1.1. *A selection of stent designs.*

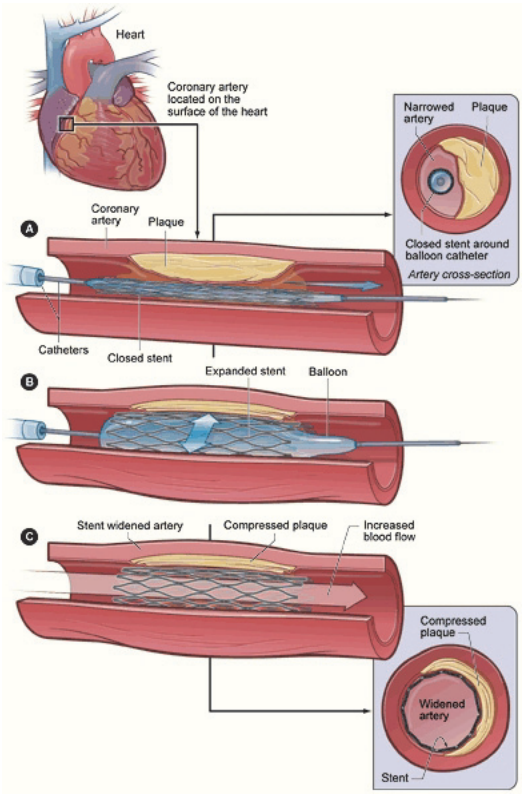

FIG. 1.2. *The illustration shows a cross-section of a coronary artery with plaque buildup. The coronary artery is located on the surface of the heart. In* A *we see the deflated balloon catheter inserted into the narrowed coronary artery. In* B*, the balloon is inflated, compressing the plaque and restoring the size of the artery. Finally,* C *shows the widened artery. (Source: National Heart, Lung, and Blood Institute; National Institutes of Health; U.S. Department of Health and Human Services.)*

with incomplete healing of the artery, and substantial efforts are now dedicated to the development of enhanced DESs. Photographs of typical stent designs are provided in Figure 1.1, while Figure 1.2 displays the stent *in situ* in the coronary artery.

An important aspect in the performance of any DES is the drug release profile. Although a number of animal models are recommended for preclinical safety and efficacy evaluation of these devices [38], incomplete understanding of the factors governing drug release and distribution following stenting currently limits the

optimization of such drug release profiles. Several authors have focused specifically on the drug release problem. Zhao et al. [45] presented an analytical solution of a cylindrical diffusion model to describe the experimental drug release of everolimus from a Dynalink-E polymer coated stent. They demonstrated that the release could be controlled by varying the coating thickness and diffusion coefficient and found that their model solution could be fitted to both *in vitro* and *in vivo* data simply by varying the diffusion coefficient. Formaggia, Minisini, and Zunino [15] considered a dissolution-diffusion model which also incorporated polymer degradation, while Prabhu and Hussainy [36] focused specifically on the degradation and release of everolimus from a polylactic stent coating and validated their compartmentalized model using *in vitro* data. A number of other contributions in the literature have attempted to combine mathematical modeling with experimental validation. Balakrishnan et al. [2] utilized computational fluid dynamics and two-dimensional transient convection-diffusion to make predictions of drug elution which were then verified using empirical data from stented porcine arteries. They found that arterial uptake was only maximized when the rates of drug release and absorptions matched. Rossi et al. [37] modeled a bioresorbable DES based on detailed constitutive equations and taking into account the main physical and chemical mechanisms involved in coating degradation, drug release, and restenosis inhibition. Their results were verified against selected *in vitro* and *in vivo* data available in the literature. Most recently, Tzafriri et al. [42] developed a mathematical framework of arterial drug distribution and receptor binding following stent elution. Their model predicted that tissue content linearly tracked stent elution rate; this prediction was validated in porcine coronary artery sirolimus-eluting polymer coated stent implants. In an attempt to make some gains in modeling this complex problem, Seidlitz et al. [39] utilized a vessel-simulating flow through cell to examine release from DES *in vitro*. This tool allowed for the examination of diffusion depth and the distribution in the arterial wall.

Several computational approaches to drug release from stents have been employed. Lovich and Edelman [28], Constantini, Maceri, and Vairo [10], and McGinty et al. [30] numerically studied a one-dimensional model. Two-dimensional models were computed by Hwang, Wu, and Edelman [20], Zunino [47], and Grassi et al. [16]. A three-dimensional model in a simplified geometry was studied by Hose et al. [19], while Vairo et al. [43] considered a multidomain approach. Zunino et al. [48] presented three-dimensional numerical models of stent expansion and release into the blood flow and tissue, while the effect of luminal flow on arterial deposition is considered in [23] and [24]. Karner and Perktold [21] used the finite element method to calculate the transport processes across the lumen, the intima, and the media, coupled with the flux across the endothelium and the internal elastic lamina, which they modeled mathematically using the Kedem–Katchalsky equations. Delfour, Garon, and Longo [14], on the other hand, focused on the effect of the number of struts and the ratio between the coated area, and attempted to optimize the effect of the dose. Mongrain et al. [31] numerically investigated the effect of diffusion coefficient and struts apposition on drug accumulation in the arterial wall. More recently, Tambača et al. [41] presented a mathematical model for the study of the mechanical properties of endovascular stents in their expanded state. Realizing the sheer complexity of modeling the whole stent-tissue system, D'Angelo et al. [13] employed model reduction strategies to simplify the computations. This involved a combination of lumped parameter models to account for drug release, a one-dimensional model to handle the complex stent pattern, and a three-dimensional model for drug transfer in the artery.

Despite the aforementioned numerical advances, there is still a lack of analytical

solutions in the literature, especially for the coupled stent-tissue system. Two interesting papers by Pontrelli and de Monte [33], [34] considered a similar model to the more general (but still one-dimensional) models of McGinty et al. [30]. Their model is a two-layer model (drug concentration in both the polymer and the tissue regions) and, through the Kedem–Katchalsky equations, allows for a topcoat. They obtained an elegant analytical solution through separation of variables and used this solution to show the effect of filtration velocity, drug metabolism, and the amount (i.e., the mass) of drug in the tissue. Pontrelli and de Monte have subsequently extended their work to consider a multilayer model [35]. Mathematical models which admit analytical solutions, such as the one considered in this paper, have a real part to play in addressing this complex problem.

This paper develops a mathematical model for drug release from polymer coated DESs and the subsequent uptake into the arterial wall. Having written a model which makes certain simplifying assumptions, the strategy is the following. First, we assume that we know the drug release concentration at the interface between the polymer and the tissue, say $g(t)$. This allows us to obtain a general analytical solution for any $g(t)$ both for the drug concentration in the extracellular matrix and the smooth muscle cells themselves. This analytical solution involves the inversion of a Laplace transform with three branch points. We then examine the concentration in the polymer and observe that, if $g(t)$ were known, the problem would be over-determined. Indeed, we can write two independent well-posed problems, both of which admit analytical solutions. However, the arbitrary function $g(t)$, representing drug release, must be such that the two solutions are identical. Hence, by equating these two solutions, it is possible to derive a Volterra integral equation for $g(t)$. We then proceed to solve this integral equation for $g(t)$ and utilize this in computing the mass of drug in the cells and extracellular space. Thus we have an alternative approach to the two-layered model of Pontrelli and de Monte that is capable of modeling the drug concentration within the target smooth muscle cells, which is what clinicians are principally interested in. This is a novel approach to solving this problem and, moreover, can be regarded as a generic mathematical tool for solving these types of diffusion systems.

2. The structure of the arterial wall. The arterial wall is a heterogeneous structure consisting of three distinct layers: the intima, the media, and the adventitia [44]; see Figure 2.1. The intima is the innermost region closest to the lumen. The main constituent of the intima is the endothelial layer of cells, known as the endothelium. This layer is crucial to the control of the normal function of the artery, through its mediation of relaxation and contraction and via its control of smooth muscle cell proliferation within the underlying media layer. The internal elastic lamina (a fenestrated layer of elastic tissue) forms the outermost part of the intima. The next layer is the media (middle) region containing smooth muscle cells, collagen, and elastin. Finally, the outermost layer of the arterial wall is the adventitia, which is separated from the media by the external elastic lamina. Essentially, the adventitia tethers the artery to perivascular tissue and contains cells known as fibroblasts. There is also the presence of a network of small blood vessels, termed vasa vasorum, which act as a blood supply to the adventitia and provide a clearance mechanism for drugs released into the artery wall.

3. The mathematical model. To obtain a tractable mathematical model we make certain assumptions about the structure of the arterial wall. The intima, when it is devoid of the endothelium, has a structure similar to that of the media region, and for this reason we shall not include the intima as a separate region in the model.

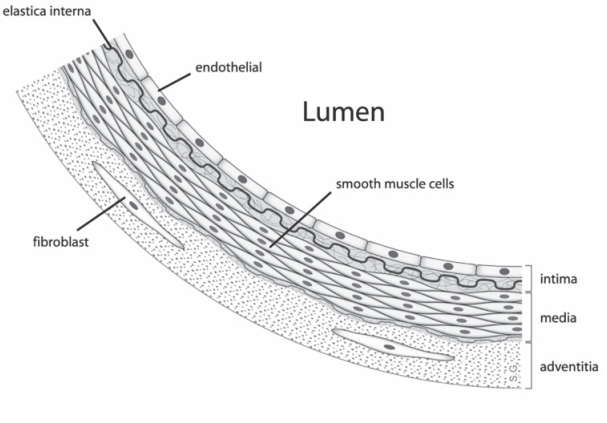

FIG. 2.1. *The structure of the arterial wall.*

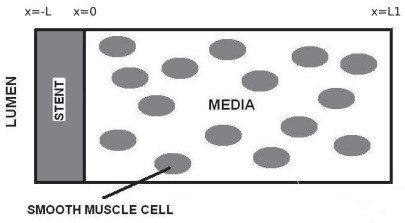

FIG. 3.1. *Simplified geometry displaying stent impinged against media region containing smooth muscle cells and extracellular space.*

Second, the adventitia is omitted, since there is some evidence in the literature [30] that the adventitia does not have a large effect on the cellular drug concentration in the media region. The media consists of two phases: one of smooth muscle cells, and the other of collagen and elastin surrounded by an interstitial (or extracellular) region. We treat the media as a porous region, where the porosity, $\phi \in (0, 1)$, is defined as the ratio of the volume of interstitial space to the total volume. The drug is known to have a partition coefficient, K, that is, the equilibrium ratio of concentrations of a compound in two different phases, and we regard the drug as interacting with the cells but not diffusing within them. It is well accepted (see, for example, [3]) that there is a transmural flow of plasma across the intima and through the media causing the drug to convect. We shall assume that the velocity of this flow, v, is constant. The purpose of including the drug within the stent is to target, and hence inhibit, the smooth muscle cells which constitute the neointima. Figure 3.1 provides a diagrammatic sketch of the simplified physiology of the artery wall. Of course, these assumptions are somewhat gross, but they do have the advantage that they allow some progress toward an analytical solution rather than a purely numerical one.

We consider a stent coated with a thin layer (of thickness L) of polymer containing a drug and embedded into the arterial wall (of thickness L_1) as schematically illustrated in Figure 3.1. We introduce $c_1(x, t)$ and $c_2(x, t)$ which denote, respectively, the concentration of the drug in the interstitial region (of the media) and the concentration of the drug within the cells. The drug concentration in the polymer,

$c(x,t)$, is assumed to satisfy a diffusion equation with diffusion coefficient D, while the transport of drug through the media is governed by an advection-diffusion equation where the transmural velocity of the plasma is denoted by v, and D_1 denotes the drug diffusion coefficient through the interstitial region. We include an uptake equation, with drug uptake rate constant α, to describe the uptake of drug into the cells within the tissue. The mathematical model is

$$\frac{\partial c}{\partial t} = D\,\frac{\partial^2 c}{\partial x^2}\,, \quad x \in (-L,0),\ t>0, \tag{3.1}$$

$$D\,\frac{\partial c}{\partial x} = 0, \quad x = -L,\ t>0, \tag{3.2}$$

$$c = c_0, \quad x \in [-L,0],\ t=0, \tag{3.3}$$

$$D\,\frac{\partial c}{\partial x} = D_1 \frac{\partial c_1}{\partial x} - v c_1, \quad x=0,\ t>0, \tag{3.4}$$

$$-D\,\frac{\partial c}{\partial x} = P(c-c_1), \quad x=0,\ t>0, \tag{3.5}$$

$$\phi\frac{\partial c_1}{\partial t} + v\,\frac{\partial c_1}{\partial x} = D_1\,\frac{\partial^2 c_1}{\partial x^2} - \alpha(c_1 - c_2/K), \quad x \in (0,L_1),\ t>0, \tag{3.6}$$

$$c_1, c_2 \text{ bounded}, \quad x \in [0,L_1],\ t \in [0,\infty), \tag{3.7}$$

$$c_1 = c_2 = 0, \quad x \in [0,L_1],\ t=0, \tag{3.8}$$

$$(1-\phi)\,\frac{\partial c_2}{\partial t} = \alpha(c_1 - c_2/K), \quad x \in (0,L_1),\ t>0. \tag{3.9}$$

This model assumes that the drug in the polymer is in a single phase which is permitted to freely diffuse. This is appropriate when the initial concentration of drug in the polymer is below solubility, in which case the dissolution of drug can be regarded as instantaneous [8]. If the initial concentration of drug in the polymer is above solubility, then the drug may exist in two forms, crystalline and dissolved, with only dissolved drug free to diffuse. An approximate solution to the problem of drug release into an infinite sink for this case is provided by Higuchi [17]. Generalizations of Higuchi's work were considered by Biscari et al. [6] and Cohen and Erneux [9]. However, in some DES systems, it may well be the case that the initial concentration of the drug in the polymer is above solubility. In this case, if diffusion is the governing step in the release process, then our assumption is still valid [40]. In this paper we focus on the polymer coated Cypher sirolimus-eluting stent (see section 6 for a description). We have conducted experiments within our laboratory which examine *in vitro* drug release from the Cypher stent. Figure 3.2 displays a comparison between the experimentally measured cumulative percentage of drug released and the widely published solution of (3.1)–(3.3) along with the condition $c = 0$ at $x = 0$ (see, for

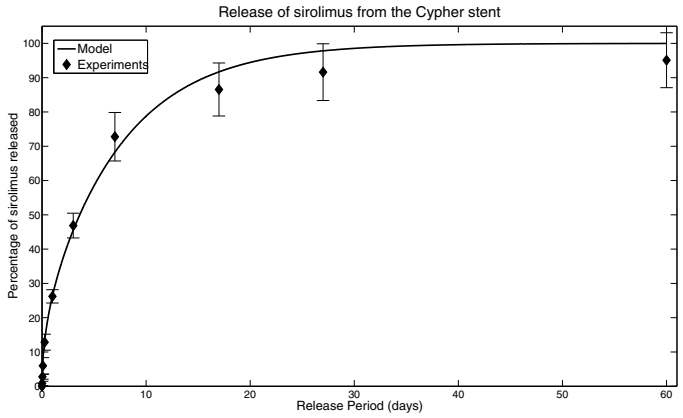

FIG. 3.2. *Comparison between* in vitro *experimental data and diffusion-based model of sirolimus release from the Cypher stent. Briefly, the experiments consisted of placing four Cypher DESs in separate sealed glass vials containing physiological release medium (phosphate buffered saline:ethanol (*90:10*)). The experiments were carried out at* 37°C. *At several time points up to* 60 *days, each stent was removed and placed in a separate vial containing fresh release medium, with the mass of drug in the original solution subsequently quantified using UV spectroscopy.*

example, Crank [12]). The good agreement between the model and the experiments serves to demonstrate that diffusion is the dominant mechanism of release, at least for this particular stent. The best-fitting value of D based on a least squares analysis was found to be of the order $10^{-16}\mathrm{m}^2\mathrm{s}^{-1}$.

We assume that the polymer rests against the bare metal of the stent, and consequently there is zero flux at $x = -L$. For simplicity the initial concentration within the polymer is assumed to be some constant c_0. At the polymer/tissue interface the total flux is assumed to be continuous, and a topcoat on the polymer is allowed via the condition (3.5) where, here, P denotes a parameter with units $m\ s^{-1}$ (see, e.g., [33]). Equation (3.6) governs the movement of the drug in the interstitial region of the media. Note that the "sink" term represents the removal of drug to the cells. Some existing models consider binding sites within the tissue (see, e.g., [42], [7]). It is certainly true that the drug will bind to binding sites in the tissue and in the cells [42], [5], [26], although the strength of affinity will likely vary substantially with the particular drug under consideration, and further, it is not clear how the density of the binding sites may be easily determined. The uptake of drug into smooth muscle cells has been measured experimentally (see, for example, [46]). The model considered here does not account for binding sites in the extracellular matrix but instead considers cells within the tissue absorbing and releasing drug as the concentration in the extracellular region changes. This idea is supported by the work in [1] and [18]. It is worth stating that no boundary condition has been stipulated at the media/adventitia interface. An argument could be made for imposing continuity of the relative diffusive and convective fluxes across the interface, or simply that the extracellular concentration falls to zero by the time the drug reaches the adventitia region. These boundary conditions, and others, have been considered in the literature (see, for example, [30], [47], [33]). However, in order to be able to obtain an analytical solution, we do not state a boundary condition at $x = L_1$, but instead impose the condition that the concentration of drug in the extracellular region and the cells must remain bounded for all x and t.

Since the system is linear, one obvious approach would be to solve directly using Laplace transforms. However, it is readily seen that this approach leads to a Laplace transform which is simply impractical to invert. Further, any attempt to proceed with the inversion would necessarily involve extremely complicated transcendental equations that must be solved for the roots. Thus we consider the following novel approach to solving this problem. Consider a simpler hypothetical problem where we assume that we know $c_1(0,t)$ in terms of a general function of t, say $g(t)$. This will allow us to obtain the concentrations for the drug in both the cells and the interstitial region (in terms of $g(t)$) and, as we shall see, reduce the problem of finding $g(t)$ to that of solving a Volterra integral equation.

We shall introduce the following nondimensional variables:

$$t' = (D_1/L_1^2)t, \quad x' = x/L_1, \quad c' = c/c_0, \quad c_1' = c_1/c_0, \quad c_2' = c_2/c_0,$$

so that the above model becomes (all primes have been omitted for reasons of clarity):

$$\frac{\partial c}{\partial t} = \delta \frac{\partial^2 c}{\partial x^2}, \quad x \in (-\ell, 0),\ t > 0, \tag{3.1$'$}$$

$$\frac{\partial c}{\partial x} = 0, \quad x = -\ell,\ t > 0, \tag{3.2$'$}$$

$$c = 1, \quad x \in [-\ell, 0],\ t = 0, \tag{3.3$'$}$$

$$\delta \frac{\partial c}{\partial x} = \frac{\partial c_1}{\partial x} - Pe\, c_1, \quad x = 0,\ t > 0, \tag{3.4$'$}$$

$$-\frac{\partial c}{\partial x} = \tilde{P}(c - c_1), \quad x = 0,\ t > 0, \tag{3.5$'$}$$

$$\phi \frac{\partial c_1}{\partial t} + Pe \frac{\partial c_1}{\partial x} = \frac{\partial^2 c_1}{\partial x^2} - Da(c_1 - c_2/K), \quad x \in (0,1),\ t > 0, \tag{3.6$'$}$$

$$c_1, c_2 \text{ bounded}, \quad x \in [0,1],\ t > 0, \tag{3.7$'$}$$

$$c_1 = c_2 = 0, \quad x \in [0,1],\ t = 0, \tag{3.8$'$}$$

$$(1-\phi)\frac{\partial c_2}{\partial t} = Da(c_1 - c_2/K), \quad x \in (0,1),\ t > 0. \tag{3.9$'$}$$

Here $\delta = D/D_1$, $\ell = L/L_1$, $\tilde{P} = L_1 P/D$, $Pe = L_1 v/D_1$ (Peclet number), and $Da = L_1^2 \alpha / D_1$ (Damkholer number).

4. An analytical solution. Consider the problem consisting of (3.6)$'$–(3.9)$'$ together with $c_1(0,t) = g(t)$. We shall now apply Laplace transforms to (3.6)$'$ and (3.9)$'$. We shall then discover, upon applying the complex inversion formula, that the integrand has three branch points, requiring a modification of the usual Bromwich contour and leading ultimately to an analytical solution in terms of the unknown drug release concentration, $g(t)$.

4.1. Solution in Laplace transform space. Rearranging (3.9)$'$ provides

$$\frac{\partial c_2}{\partial t}(x,t) + \frac{\gamma}{K} c_2(x,t) = \gamma c_1(x,t), \tag{4.1}$$

where

$$\gamma = \frac{Da}{1-\phi}.$$

Solving (4.1) subject to the initial condition gives

$$c_2(x,t) = \gamma \int_0^t e^{-\gamma(t-t')/K}\, c_1(x,t')\, dt'. \tag{4.2}$$

After substituting (4.2) into (3.6)′, we obtain

$$\begin{aligned}\phi\frac{\partial c_1}{\partial t}(x,t) + Pe\frac{\partial c_1}{\partial x}(x,t) \\ = \frac{\partial^2 c_1}{\partial x^2}(x,t) - Da\left(c_1(x,t) - \frac{\gamma}{K}\int_0^t e^{-\gamma(t-t')/K}\, c_1(x,t')\, dt'\right).\end{aligned} \tag{4.3}$$

Define the Laplace transform of $c_i(x,t)$ $(i=1,2)$ with respect to t:

$$\bar{c_i}(x,s) = \int_0^\infty e^{-st}\, c_i(x,t)\, dt.$$

Now, taking Laplace transforms of (4.3) yields, after making use of the initial condition and rearranging,

$$\frac{d^2\bar{c_1}}{dx^2}(x,s) - Pe\frac{d\bar{c_1}}{dx}(x,s) - \Gamma(s)\bar{c_1}(x,s) = 0, \tag{4.4}$$

where

$$\Gamma(s) = \frac{\phi K s\left(s + \frac{\gamma}{K} + \frac{Da}{\phi}\right)}{Ks + \gamma}. \tag{4.5}$$

Solving (4.4) subject to $c_1(0,t) = g(t)$ and the boundedness of $c_1(x,t)$, we obtain

$$\bar{c_1}(x,s) = \bar{g}(s)\ \exp\left\{\frac{xPe}{2}\right\}\ \exp\left\{-\frac{x}{2}\sqrt{Pe^2 + 4\Gamma(s)}\right\}, \tag{4.6}$$

where $\bar{g}(s) = \int_0^\infty e^{-st}g(t)dt$. Using the definition of $\Gamma(s)$ from (4.5), it is possible to rewrite (4.6) in a more transparent form which clearly displays the dependence on s:

$$\bar{c_1}(x,s) = \bar{g}(s)\ \exp\left\{\frac{xPe}{2}\right\}\ \exp\left\{-x\sqrt{\phi}\sqrt{\frac{(s+s_1)\,(s+s_2)}{s+s_3}}\right\}, \tag{4.7}$$

where

$$2s_{1,2} = \frac{\gamma}{K} + \frac{Da}{\phi} + \frac{Pe^2}{4\phi} \mp \sqrt{\left(\frac{\gamma}{K} + \frac{Da}{\phi} + \frac{Pe^2}{4\phi}\right)^2 - \frac{\gamma Pe^2}{\phi K}}, \tag{4.8}$$

$$s_3 = \frac{\gamma}{K}. \tag{4.9}$$

Finally, taking the Laplace transform of (4.2) (and using convolution) allows us to write the solution of c_2 in Laplace transform space:

$$\begin{aligned}\bar{c_2}(x,s) &= \frac{\gamma}{s+s_3}\,\bar{c_1}(x,s) \\ &= \frac{\gamma\bar{g}(s)}{(s+s_3)}\exp\left\{\frac{xPe}{2}\right\}\ \exp\left\{-x\sqrt{\phi}\sqrt{\frac{(s+s_1)\,(s+s_2)}{s+s_3}}\right\}.\end{aligned} \tag{4.10}$$

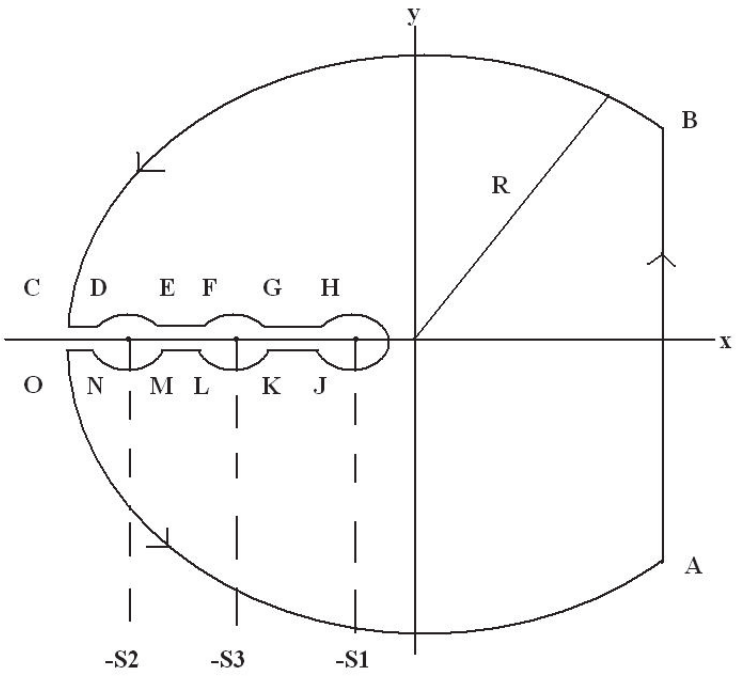

FIG. 4.1. *Modified Bromwich contour. Note that the circles centered on* $-s_1$, $-s_3$, *and* $-s_2$ *have radii* ϵ_1, ϵ_3, *and* ϵ_2, *respectively.* $A, B, \ldots, N, O$ *are defined in the appendix.*

4.2. Solution via complex inversion formula. It will be convenient first to determine the inverse of the Laplace transform

$$\bar{f}(s) = \frac{\exp\left\{-x\sqrt{\phi}\sqrt{\frac{(s+s_1)(s+s_2)}{(s+s_3)}}\right\}}{s}; \tag{4.11}$$

that is, by the complex inversion formula, we require

$$f(t) = L^{-1}[\bar{f}(s)] = \frac{1}{2\pi i}\int_{\beta-i\infty}^{\beta+i\infty} \frac{\exp\left\{st - x\sqrt{\phi}\sqrt{\frac{(s+s_1)(s+s_2)}{(s+s_3)}}\right\}}{s} ds. \tag{4.12}$$

To evaluate (4.12) we consider the modified Bromwich contour in Figure 4.1. We observe that the integrand of (4.12) has a simple pole at $s = 0$ and three branch points at $-s_1, -s_3$, and $-s_2$. We shall later demonstrate that the typical values of the parameters characterizing the model are such that $0 < s_1 < s_3 < s_2$. Thus a branch cut has been made along the negative real axis. The details of the inversion are provided in the appendix. The solution $f(t)$ turns out to be

$$f(t) = \exp\left\{-x\sqrt{\frac{\phi s_1 s_2}{s_3}}\right\} - \frac{1}{\pi}(I_1 + \tilde{I}_1), \tag{4.13}$$

where

$$I_1 = \int_{s_2}^{\infty} \frac{e^{-ut}\sin(a(u)x)}{u}\, du, \quad \tilde{I}_1 = \int_{s_1}^{s_3} \frac{e^{-ut}\sin(a(u)x)}{u}\, du, \tag{4.14}$$

with

$$a(u) = \sqrt{\frac{\phi(u-s_1)(u-s_2)}{(u-s_3)}}\,. \tag{4.15}$$

Note that we can rewrite (4.7) as

$$\bar{c_1}(x,s) = \exp\left(\frac{xPe}{2}\right)\; s\;\bar{g}(s)\;\bar{f}(s). \tag{4.16}$$

An application of the convolution theorem to (4.16) and integration by parts results in

(4.17)

$$c_1(x,t) = \exp\left(\frac{xPe}{2}\right)\left[g(t)\exp\left\{-x\sqrt{\frac{\phi s_1 s_2}{s_3}}\right\} - \frac{g(t)\left(I_2+\tilde{I}_2\right)}{\pi} + \frac{I_3+\tilde{I}_3}{\pi}\right],$$

where

$$I_2 = \int_{s_2}^{\infty}\frac{\sin(a(u)x)}{u}\,du, \quad \tilde{I}_2 = \int_{s_1}^{s_3}\frac{\sin(a(u)x)}{u}\,du$$

and

$$I_3 = \int_{s_2}^{\infty}\int_0^t g(t')e^{-u(t-t')}\sin(a(u)x)\,dt'du,$$
$$\tilde{I}_3 = \int_{s_1}^{s_3}\int_0^t g(t')e^{-u(t-t')}\sin(a(u)x)\,dt'du.$$

A further application of the convolution theorem to (4.11) then yields

$$c_2(x,t) = \gamma\exp\left(\frac{xPe}{2}\right)\left[\exp\left\{-x\sqrt{\frac{\phi s_1 s_2}{s_3}}\right\}I_4 - \frac{I_5+\tilde{I}_5}{\pi} + \frac{I_6+\tilde{I}_6}{\pi}\right], \tag{4.18}$$

where

$$I_4 = \int_0^t g(t')e^{-s_3(t-t')}dt',$$
$$I_5 = \int_{s_2}^{\infty}\int_0^t g(t')e^{-s_3(t-t')}\frac{\sin(a(u)x)}{u}\,dt'du,$$
$$\tilde{I}_5 = \int_{s_1}^{s_3}\int_0^t g(t')e^{-s_3(t-t')}\frac{\sin(a(u)x)}{u}\,dt'du$$

and

$$I_6 = \int_{s_2}^{\infty}\int_0^t\int_0^{\tau} g(t')e^{-u(\tau-t')}e^{-s_3(t-\tau)}\sin(a(u)x)\,dt'd\tau du,$$

$$\tilde{I}_6 = \int_{s_1}^{s_3}\int_0^t\int_0^{\tau} g(t')e^{-u(\tau-t')}e^{-s_3(t-\tau)}\sin(a(u)x)\,dt'd\tau du.$$

5. A Volterra integral equation. We have obtained $c_1(x,t)$ and $c_2(x,t)$ in terms of the arbitrary function $g(t)$. The object now is to determine $g(t)$. Consider the problem

$$\frac{\partial c}{\partial t} = \delta \frac{\partial^2 c}{\partial x^2}, \quad x \in (-\ell, 0),\ t > 0, \tag{5.1}$$

$$\frac{\partial c}{\partial x} = 0, \quad x = -\ell,\ t > 0, \tag{5.2}$$

$$c = 1, \quad x \in [-\ell, 0],\ t = 0, \tag{5.3}$$

$$\delta \frac{\partial c}{\partial x} = \frac{\partial c_1}{\partial x} - Pe\, c_1, \quad x = 0,\ t > 0, \tag{5.4}$$

$$-\frac{\partial c}{\partial x} = \tilde{P}(c - c_1), \quad x = 0,\ t > 0, \tag{5.5}$$

where we intend to replace $c_1(0,t)$ by $g(t)$. If we were able to determine $\partial c_1(0,t)/\partial x$ (and hence $\partial c(0,t)/\partial x$), then (5.1)–(5.5) would be overdetermined. This "overdeterminedness" could then be used to find an expression for $g(t)$. However, it is not difficult to see that $\partial c_1(0,t)/\partial x$ is not defined: this is a direct consequence of the discontinuity in the boundary and initial condition at $x = 0$ and $t = 0$ of the model defined by (3.1)–(3.9). A form of regularization is required. We have chosen to approximate $\partial c_1(0,t)/\partial x$ by utilizing the solution of the corresponding problem of pure diffusion in a semi-infinite composite region. To be precise here, we mean the solution obtained by solving (3.1)′–(3.7)′, where $[0,1]$ has been replaced by $[0,\infty)$, $\phi = 1$, and Pe and Da have been taken to be zero. It can be readily shown that, in this case,

$$\begin{aligned}\frac{\partial c_1(0,t)}{\partial x} &= \frac{\tilde{P}\sqrt{\delta}}{\pi} \int_0^\infty \frac{B \sin\left(l\sqrt{u/\delta}\right) \exp(-ut)}{\sqrt{u}\,(A^2 + B^2)}\, du, \\ &= j(t),\ \text{say},\end{aligned}$$

where

$$A = \tilde{P} \cos\left(l\sqrt{u/\delta}\right) - \left(\sqrt{u/\delta}\right) \sin\left(l\sqrt{u/\delta}\right)$$

and

$$B = \tilde{P}\sqrt{\delta} \sin\left(l\sqrt{u/\delta}\right).$$

Thus, we regularize by replacing (5.4) by

$$\delta \frac{\partial c}{\partial x} = j(t) - Pe\, c_1, \quad x = 0,\ t > 0. \tag{5.6}$$

Consider the further transformation of the independent variables

$$t' = (\delta/\ell^2)t, \quad x' = \left(\frac{x + \ell}{\ell}\right), \tag{5.7}$$

so that (5.1)–(5.3), (5.5), and (5.6) become

$$\frac{\partial c}{\partial t} = \frac{\partial^2 c}{\partial x^2}, \quad x \in (0,1),\ t > 0, \tag{5.8}$$

$$\frac{\partial c}{\partial x} = 0, \quad x = 0,\ t > 0, \tag{5.9}$$

$$c = 1, \quad x \in [0,1],\ t = 0, \tag{5.10}$$

$$\frac{\partial c}{\partial x} = \frac{\ell}{\delta} j(t) - \frac{\ell P_e}{\delta} g(t), \quad x = 1,\ t > 0, \tag{5.11}$$

$$-\frac{\partial c}{\partial x} = P^*(c - g(t)), \quad x = 1,\ t > 0, \tag{5.12}$$

where $P^* = \ell \tilde{P} = LP/D$. Again, the primes have been omitted for clarity. We are now in a position to write two problems and their associated solutions.

Problem 1.

$$\frac{\partial c}{\partial t} = \frac{\partial^2 c}{\partial x^2}, \quad x \in (0,1),\ t > 0, \tag{5.13}$$

$$\frac{\partial c}{\partial x} = 0, \quad x = 0,\ t > 0, \tag{5.14}$$

$$c = 1, \quad x \in [0,1],\ t = 0, \tag{5.15}$$

$$\frac{\partial c}{\partial x} = \frac{\ell}{\delta} j(t) - \frac{\ell P_e}{\delta} g(t), \quad x = 1,\ t > 0. \tag{5.16}$$

The following solution may be obtained from either an application of Laplace transforms or separation of variables with Duhamel's theorem:

$$c(x,t) = 1 - \frac{\ell}{\delta} \int_0^t (P_e\, g(\tau) - j(\tau)) \left[1 + 2 \sum_{n=1}^{\infty} (-1)^n \exp(-n^2 \pi^2 (t-\tau)) \cos(n\pi x) \right] d\tau. \tag{5.17}$$

Problem 2.

$$\frac{\partial c}{\partial t} = \frac{\partial^2 c}{\partial x^2}, \quad x \in (0,1),\ t > 0, \tag{5.18}$$

$$\frac{\partial c}{\partial x} = 0, \quad x = 0,\ t > 0, \tag{5.19}$$

$$c = 1, \quad x \in [0,1],\ t = 0, \tag{5.20}$$

$$-\frac{\partial c}{\partial c} = P^*(c - g(t)), \quad x = 1,\ t > 0. \tag{5.21}$$

In a similar manner the following solution may be obtained:

$$c(x,t) = 2P^* \sum_{n=0}^{\infty} \frac{\exp(-\xi_n^2 t) \cos(\xi_n x)}{\xi_n [(1+P^*) \sin \xi_n + \xi_n \cos \xi_n]} + 2P^* \int_0^t g(\tau) \sum_{n=0}^{\infty} \frac{\xi_n \exp(-\xi^2 (t-\tau)) \cos(\xi_n x)}{[(1+P^*) \sin \xi_n + \xi_n \cos \xi_n]} d\tau, \tag{5.22}$$

where $\xi_n,\ n = 0, 1, 2, \ldots$, are the countably infinite roots of

$$\xi \tan \xi = P^*. \tag{5.23}$$

The two solutions (5.17) and (5.22) must be identical, i.e., valid for all values of $x \in [0,1]$ and $t > 0$. We shall elect to equate the two integrals (over x) of (5.17) and (5.22). The physical significance of this is that we are effectively equating the respective expressions for the mass of drug on the stent. Thus

$$\begin{aligned}
&2P^* \sum_{n=0}^{\infty} \frac{\exp(-\xi_n^2\, t)}{\xi_n[(1+P^*)\sin\xi_n + \xi_n\cos\xi_n]} \int_0^1 \cos(\xi_n\, x)dx \\
&\quad + 2P^* \int_0^t g(\tau) \sum_{n=0}^{\infty} \frac{\xi_n \exp(-\xi_n^2(t-\tau))}{[(1+P^*)\sin\xi_n + \xi_n\cos\xi_n]} \int_0^1 \cos(\xi_n\, x)dx\; d\tau \\
&= 1 - \frac{\ell}{\delta}\int_0^t (P_e\; g(\tau) - j(\tau)) \left[1 + 2\sum_{n=1}^{\infty}(-1)^n \exp(-n^2\pi^2(t-\tau)) \int_0^1 \cos(n\pi x)dx\right] d\tau,
\end{aligned}$$

and so

$$\begin{aligned}
&2P^* \quad \sum_{n=0}^{\infty} \frac{\exp(-\xi_n^2\, t)\sin\xi_n}{\xi_n^2[(1+P^*)\sin\xi_n + \xi_n\cos\xi_n]} \\
&\qquad + 2P^* \int_0^t g(\tau) \sum_{n=0}^{\infty} \frac{\exp(-\xi_n^2(t-\tau))\sin\xi_n}{[(1+P^*)\sin\xi_n + \xi_n\cos\xi_n]} d\tau \\
&\qquad = 1 - \frac{\ell}{\delta}\int_0^t (P_e\; g(\tau) - j(\tau))\, d\tau.
\end{aligned} \tag{5.24}$$

Differentiating with respect to t gives

$$\begin{aligned}
&-2P^* \sum_{n=0}^{\infty} \frac{\exp(-\xi_n^2\, t)\sin\xi_n}{[(1+P^*)\sin\xi_n + \xi_n\cos\xi_n]} + 2P^* \left(g(t) \sum_{n=0}^{\infty} \frac{\sin\xi_n}{[(1+P^*)\sin\xi_n + \xi_n\cos\xi_n]} \right. \\
&\qquad \left. - \int_0^t g(t) \sum_{n=0}^{\infty} \frac{\xi_n^2 \exp(-\xi_n^2(t-\tau))\sin\xi_n}{[(1+P^*)\sin\xi_n + \xi_n\cos\xi_n]} d\tau \right)
\end{aligned} \tag{5.25}$$

$$= -\frac{\ell}{\delta}\left(P_e\; g(t) - j(t)\right).$$

Rearranging yields

$$\begin{aligned}
&\left\{ 2P^* \sum_{n=0}^{\infty} \frac{\sin\xi_n}{[(1+P^*)\sin\xi_n + \xi_n\cos\xi_n]} + \frac{\ell P_e}{\delta} \right\} g(t) \\
&\qquad = \int_0^t \left\{ 2P^* \sum_{n=0}^{\infty} \frac{\xi_n^2 \exp(-\xi_n^2(t-\tau))\sin\xi_n}{[(1+P^*)\sin\xi_n + \xi_n\cos\xi_n]} \right\} g(\tau) d\tau \\
&\qquad\quad + 2P^* \sum_{n=0}^{\infty} \frac{\exp(-\xi_n^2\, t)\sin\xi_n}{[(1+P^*)\sin\xi_n + \xi_n\cos\xi_n]} + \frac{\ell}{\delta} j(t).
\end{aligned} \tag{5.26}$$

Solving this integral equation for $g(t)$ allows us to determine $c_1(x,t)$ and $c_2(x,t)$

TABLE 6.1
Table of parameter values based on McGinty et al. [30]*, Tzafriri et al.* [42]*, and Pontrelli and de Monte* [33]*,* [34].

Parameter	Symbol	Value
Media porosity	ϕ	0.61
Media thickness	L_1	4.5×10^{-4}m
Media diffusion coefficient	D_1	$2.5 \times 10^{-10}\mathrm{m}^2\mathrm{s}^{-1}$
Drug uptake rate constant	α	$2 \times 10^{-5}\mathrm{s}^{-1}$
Partition coefficient	K	15
Transmural velocity	v	$5.8 \times 10^{-8}\mathrm{ms}^{-1}$
Polymer diffusion coefficient	D	$10^{-16}\mathrm{m}^2\mathrm{s}^{-1}$
Permeability of topcoat	P	$10^{-8}\mathrm{ms}^{-1}$
Polymer thickness	L	1.26×10^{-5}m

through the analytical solutions obtained in section 4. The concentration of drug within the polymer may then be obtained from either (5.17) or (5.22).

6. Parameter values. A common difficulty when modeling physiological processes is in obtaining estimates of the model parameters. Experimentation is often prohibitively expensive or simply not possible *in vivo*, and it is therefore usual to draw data from different studies in the literature. We refer the reader to [30], where an extensive literature search was performed to obtain estimates of the various parameters associated with drug elution from stents into arterial tissue. In this paper we will consider the nonerodible polymer coated Cypher sirolimus-eluting stent. We have chosen this particular stent system because it contains a drug-filled polymer coating and the mechanism of release is generally accepted to be diffusion. Thus this stent is well suited to our modeling assumptions. The Cypher stent coating is a blend of polyethylene-co-vinyl acetate (PEVA), poly-n-butyl methacrylate (PBMA), and the drug sirolimus. The coating is applied on a poly-o-chloro-p-xylylene (parylene-C) treated stainless steel stent. The manufacture of the Cypher consists of applying a basecoat solution containing PEVA, PBMA, and the drug. An inactive topcoat and toulene spray are then applied. As a result of the mixing and drying process, the drug is actually transported to the topcoat layer so that the drug-free topcoat is never actually realized [4]. Most of the newer generation stents also make use of limus compounds [22]. To consider different compounds in our model, we would simply require measurements of the drug-dependent parameters. The value of media porosity is taken directly from [30]. The polymer thickness is taken from [11] and the diffusion coefficient of sirolimus in the Cypher stent has been measured in our laboratory to be of order $10^{-16}\mathrm{m}^2\mathrm{s}^{-1}$, while the values of the media diffusion coefficient of sirolimus, media thickness, and transmural velocity have been taken from [42]. The value of the parameter P has been taken from [33], while the values of the drug uptake constant and partition coefficient of sirolimus have been estimated based on [30]. Using the parameter values in Table 6.1, we find that $s_1 = 3.7010 \times 10^{-4}$, $s_2 = 0.0334$, $s_3 = 0.0028$ to four decimal places, satisfying $0 < s_1 < s_3 < s_2$.

7. Solution of the integral equation. Consider the discretization $\{t_m = mh, h = T/M, m = 0, 1, \ldots, M\}$ and the associated vector $(g_0, g_1, \ldots, g_m)$ approximating $(g(0), g(t_1), \ldots, g(t_m))$. We employ an explicit Euler-type method,

$$\begin{aligned}
&\left\{2P^*\sum_{n=0}^{\infty}\frac{\sin\xi_n}{[(1+P^*)\sin\xi_n+\xi_n\cos\xi_n]}+\frac{\ell P_e}{\delta}\right\}g_m\\
&\quad=h\sum_{j=0}^{m-1}\left\{2P^*\sum_{n=0}^{\infty}\frac{\xi_n^2\exp(-\xi_n^2(m-j)h)\sin\xi_n}{[(1+P^*)\sin\xi_n+\xi_n\cos\xi_n]}\right\}g_j\\
&\qquad+2P^*\sum_{n=0}^{\infty}\frac{\exp(-\xi_n^2 mh)\sin\xi_n}{[(1+P^*)\sin\xi_n+\xi_n\cos\xi_n]}+\frac{\ell}{\delta}W_m,
\end{aligned}\tag{7.1}$$

with

$$g_0=g(0)=\frac{2P^*\Psi(\boldsymbol{\xi})+\ell W_0/\delta}{2P^*\Psi(\boldsymbol{\xi})+\frac{\ell Pe}{\delta}},\tag{7.2}$$

where

$$\Psi(\boldsymbol{\xi})=\sum_{n=0}^{\infty}\frac{\sin\xi_n}{[(1+P^*)\sin\xi_n+\xi_n\cos\xi_n]}\,.$$

Before the discrete equation (7.1) can be solved, the roots of $\xi\tan\xi=P^*$ are required. These have been obtained using a bisection approach. The infinite sums in (7.1) were truncated after the first 20 terms and then, using the calculated roots, the finite difference equation (7.1) was solved. Figure 7.1 displays $g(t)=c_1(0,t)$ over the first day.

Now that $g(t)$ has been obtained, we can utilize this $g(t)$ in solution (4.17) and (4.18) to obtain the concentration of drug in the extracellular and cellular regions, and these are displayed in Figures 7.2 and 7.3.

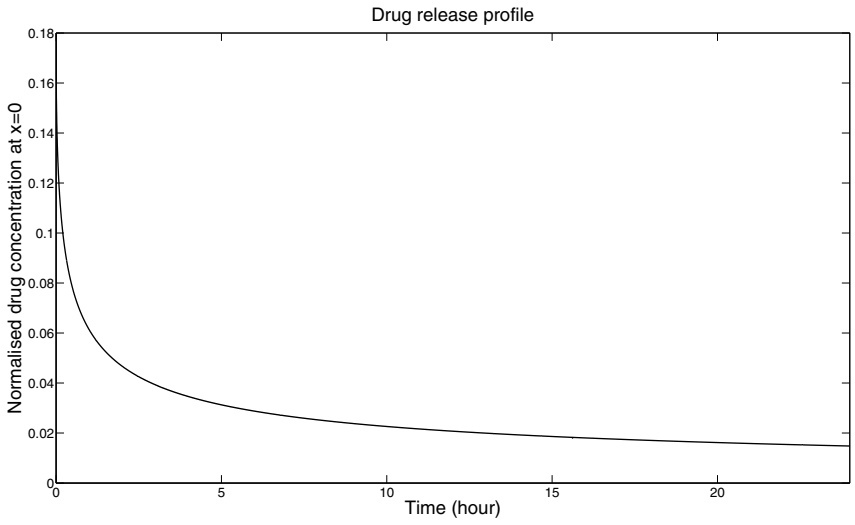

FIG. 7.1. $g(t)=c_1(0,t)$ *over the first day as calculated from* (5.26).

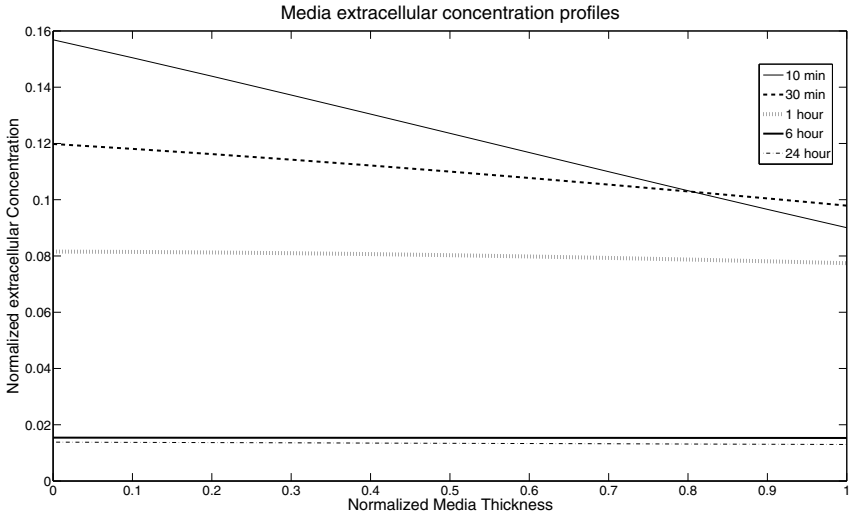

FIG. 7.2. *Variation in extracellular concentration with time, subject to $g(t)$ obtained from the solution of the Volterra integral equation.*

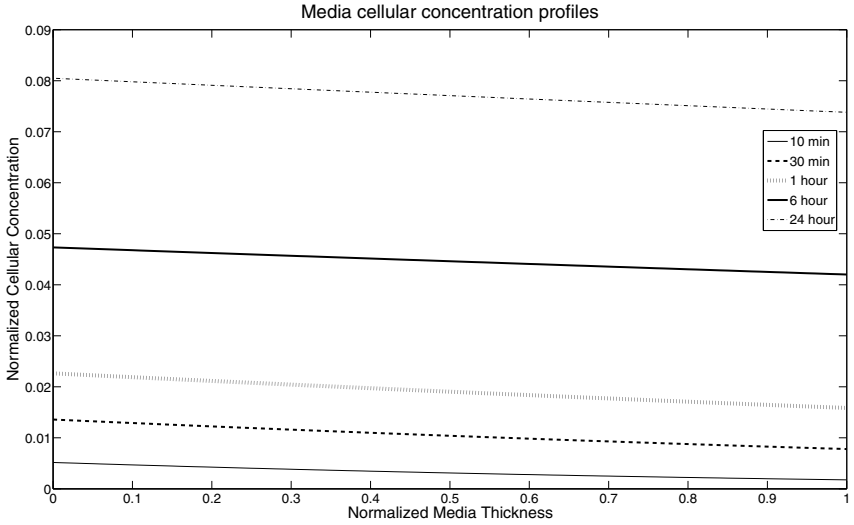

FIG. 7.3. *Variation in cellular concentration with time, subject to $g(t)$ obtained from the solution of the Volterra integral equation.*

8. Drug mass within the tissue. The total mass of drug in the media region at time t is given by integrating the expressions for cellular and extracellular concentration over the length of the media. In nondimensional terms, this equates to

$$M(t) = \int_0^1 \phi\, c_1(x,t)\, dx + \int_0^1 (1-\phi)\, c_2(x,t)\, dx. \tag{8.1}$$

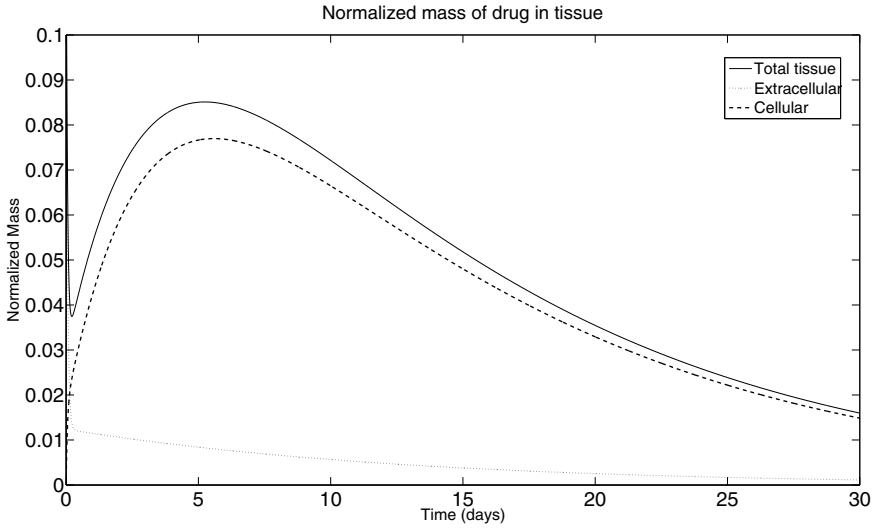

FIG. 8.1. *Variation in mass of drug in the media with time, subject to $g(t)$ obtained from the solution of the Volterra integral equation.*

Again, for convenience, the primes are suppressed.

Figure 8.1 displays the variation in mass of drug within the tissue over a period of 10 days following stent deployment, using high-order global adaptive quadrature to evaluate the integrals. We see that most of the mass is contained within the cells, due to the high partition coefficient of the drug. We have made two further assumptions in producing these plots. First, it is assumed that all of the drug is eluted from the stent, i.e., no drug is retained within the polymer. There is some evidence in the literature that for some drug-eluting stents, not all of the drug is eluted, and in fact some of the drug remains trapped in the stent. An example of such a stent is the paclitaxel-eluting Taxus stent, which is also a polymer coated stent. Experiments in our laboratory have revealed that for the sirolimus coated Cypher stent, at least 99% of the drug is eluted *in vitro* within the first three months, which justifies this assumption. The second assumption is that all of the drug released from the stent diffuses into the tissue. This assumption may be reasonable when the stent protrudes into the arterial wall.

9. Concluding remarks. In this paper we have developed analytical solutions for release of a drug from a polymer coated stent into the arterial wall. By assuming initially that the drug release concentration at the polymer/tissue interface, $g(t)$, is known, we have been able to derive a Volterra integral equation, which allows us to consider $g(t)$ as a variable of our model. Upon solving the integral equation for $g(t)$, we have been able to determine the drug concentration profiles in the extracellular and cellular regions of the arterial wall. Furthermore, we have calculated the mass of drug in each region over the period of release.

We feel it appropriate to comment on the limitations of our model. We have considered a one-dimensional model which, while making it difficult to generate quantitative results, nonetheless allows us to obtain qualitative results. However, primarily due to the regularization, there is a negligible amount of mass loss. Furthermore,

the model assumes that the main mechanism of release is diffusion. The problem of modeling arterial stents is very much an active field of research. The process of drug release from the stent *in vitro* is still not fully understood, let alone the complex *in vivo* situation where flowing blood, pulsatility, wound healing, proliferation, migration of cells, and complex uptake/binding no doubt all play some part. While we do not claim to have addressed all these issues, we believe that simple models which can admit analytical solutions, such as the one presented here, have a part to play in addressing this complex problem.

Appendix. Solution via complex inversion formula. Consider the following integral:

$$\begin{aligned} f(t) &= \frac{1}{2\pi \mathrm{i}} \int_{\beta-\mathrm{i}\infty}^{\beta+\mathrm{i}\infty} \frac{\exp\left\{ st - x\sqrt{\phi}\sqrt{\frac{(s+s_1)(s+s_2)}{s+s_3}} \right\}}{s}\, ds \\ &= \frac{1}{2\pi \mathrm{i}} \int_{\beta-\mathrm{i}\infty}^{\beta+\mathrm{i}\infty} e^{st}\bar{f}(s) ds. \end{aligned} \tag{A.1}$$

To evaluate (A.1), consider the modified Bromwich contour in Figure 4.1. Notice that the integrand of (A.1) has a simple pole at $s = 0$ and three separate branch points at $-s_1$, $-s_3$, and $-s_2$. For the parameter values considered, it is always the case that $0 < s_1 < s_3 < s_2$. Thus a branch cut has been made along the negative real axis (see Figure 4.1).

Now,

$$\begin{aligned} &\frac{1}{2\pi \mathrm{i}} \oint_C e^{st}\bar{f}(s) ds \\ &= \frac{1}{2\pi \mathrm{i}} \int_{AB} e^{st}\bar{f}(s) ds + \frac{1}{2\pi \mathrm{i}} \int_{BC} e^{st}\bar{f}(s) ds + \frac{1}{2\pi \mathrm{i}} \int_{CD} e^{st}\bar{f}(s) ds \\ &\quad + \frac{1}{2\pi \mathrm{i}} \int_{DE} e^{st}\bar{f}(s) ds + \frac{1}{2\pi \mathrm{i}} \int_{EF} e^{st}\bar{f}(s) ds + \frac{1}{2\pi \mathrm{i}} \int_{FG} e^{st}\bar{f}(s) ds \\ &\quad + \frac{1}{2\pi \mathrm{i}} \int_{GH} e^{st}\bar{f}(s) ds + \frac{1}{2\pi \mathrm{i}} \int_{HJ} e^{st}\bar{f}(s) ds + \frac{1}{2\pi \mathrm{i}} \int_{JK} e^{st}\bar{f}(s) ds \\ &\quad + \frac{1}{2\pi \mathrm{i}} \int_{KL} e^{st}\bar{f}(s) ds + \frac{1}{2\pi \mathrm{i}} \int_{LM} e^{st}\bar{f}(s) ds + \frac{1}{2\pi \mathrm{i}} \int_{MN} e^{st}\bar{f}(s) ds \\ &\quad + \frac{1}{2\pi \mathrm{i}} \int_{NO} e^{st}\bar{f}(s) ds + \frac{1}{2\pi \mathrm{i}} \int_{OA} e^{st}\bar{f}(s) ds \\ &= Res(s = 0) \end{aligned} \tag{A.2}$$

so that there are 15 integrals to consider. It can be readily shown that as $R \to \infty$, the integrals over BC and OA vanish.

Along CD, let $s = u\, e^{i\theta}$, $\theta = \pi$, $s + s_1 = u_1\, e^{i\theta_1}$, $\theta_1 = \pi$, $s + s_2 = u_2\, e^{i\theta_2}$, $\theta_2 = \pi$, $s + s_3 = u_3\, e^{i\theta_3}$, $\theta_3 = \pi$, from $s = -R$ to $s = -s_2 - \epsilon_2$:

$$\begin{aligned} &\frac{1}{2\pi i} \int_{CD} e^{st} f(s) ds \\ &= \frac{1}{2\pi i} \int_{-R}^{-s_2-\epsilon_2} e^{st} f(s) ds \end{aligned}$$

$$
\begin{aligned}
&= \frac{1}{2\pi i}\int_R^{\epsilon_2+s_2} \frac{\exp\left\{-ut - x\sqrt{\phi}\sqrt{\frac{u_1e^{i\pi}u_2e^{i\pi}}{u_3e^{i\pi}}}\right\}}{-u}(-du)\\
&= \frac{1}{2\pi i}\int_R^{\epsilon_2+s_2} \frac{\exp\left\{-ut - ix\sqrt{\phi}\sqrt{\frac{u_1u_2}{u_3}}\right\}}{u}du,\\
&= \frac{1}{2\pi i}\int_R^{\epsilon_2+s_2} \frac{\exp\left\{-ut - ix\sqrt{\phi}\sqrt{\frac{(u-s_1)(u-s_2)}{u-s_3}}\right\}}{u}du. \qquad \text{(A.3)}
\end{aligned}
$$

Along DE, the point $-s_2$ is moved to the origin by writing $s = \epsilon_2 e^{i\theta} - s_2$, $ds = i\epsilon_2 e^{i\theta}d\theta$. Thus,

$$
\begin{aligned}
&\frac{1}{2\pi i}\int_{DE} e^{st}f(s)ds\\
&= \frac{\epsilon_2}{2\pi}\int_\pi^0 \frac{\exp\left\{\left(\epsilon_2e^{i\theta}-s_2\right)t - x\sqrt{\phi}\sqrt{\epsilon_2}e^{i\theta/2}\sqrt{\frac{\epsilon_2e^{i\theta}+s_1-s_2}{\epsilon_2e^{i\theta}-s_2+s_3}} + i\theta\right\}}{\epsilon_2e^{i\theta}-s_2}\,d\theta\\
&\to 0 \quad \text{as} \quad \epsilon_2 \to 0. \qquad \text{(A.4)}
\end{aligned}
$$

Along EF, let $s = u\,e^{i\theta}$, $\theta = \pi$, $s + s_1 = u_1\,e^{i\theta_1}$, $\theta_1 = \pi$, $s + s_2 = u_2\,e^{i\theta_2}$, $\theta_2 = 0$, $s + s_3 = u_3\,e^{i\theta_3}$, $\theta_3 = \pi$, from $s = -s_2 + \epsilon_2$ to $s = -s_3 - \epsilon_3$:

$$
\begin{aligned}
&\frac{1}{2\pi i}\int_{EF} e^{st}f(s)ds\\
&= \frac{1}{2\pi i}\int_{-s_2+\epsilon_2}^{-s_3-\epsilon_3} e^{st}f(s)ds\\
&= \frac{1}{2\pi i}\int_{s_2-\epsilon_2}^{s_3+\epsilon_3} \frac{\exp\left\{-ut - x\sqrt{\phi}\sqrt{\frac{(u-s_1)(s_2-u)}{u-s_3}}\right\}}{u}du. \qquad \text{(A.5)}
\end{aligned}
$$

Along FG, the point $-s_3$ is moved to the origin by writing $s = \epsilon_3 e^{i\theta} - s_3$, $ds = i\epsilon_3 e^{i\theta}d\theta$. Thus,

$$
\begin{aligned}
&\frac{1}{2\pi i}\int_{FG} e^{st}f(s)ds\\
&= \frac{\epsilon_3}{2\pi}\int_\pi^0 \frac{\exp\left\{\begin{array}{c}\left(\epsilon_3e^{i\theta}-s_3\right)t\\ -x\sqrt{\frac{\phi}{\epsilon_3}}e^{-i\theta/2}\sqrt{\left(\epsilon_3e^{i\theta}+s_1-s_3\right)\left(\epsilon_3e^{i\theta}-s_3+s_2\right)} + i\theta\end{array}\right\}}{\epsilon_3e^{i\theta}-s_3}\,d\theta\\
&\to 0 \quad \text{as} \quad \epsilon_3 \to 0.
\end{aligned}
\qquad \text{(A.6)}
$$

Along GH, let $s = u\,e^{i\theta}$, $\theta = \pi$, $s + s_1 = u_1\,e^{i\theta_1}$, $\theta_1 = \pi$, $s + s_2 = u_2\,e^{i\theta_2}$, $\theta_2 = 0$, $s + s_3 = u_3\,e^{i\theta_3}$, $\theta_3 = 0$, from $s = -s_3 + \epsilon_3$ to $s = -s_1 - \epsilon_1$:

$$
\begin{aligned}
&\frac{1}{2\pi i}\int_{GH} e^{st}f(s)ds\\
&= \frac{1}{2\pi i}\int_{-s_3+\epsilon_3}^{-s_1-\epsilon_1} e^{st}f(s)ds
\end{aligned}
$$

$$= \frac{1}{2\pi i}\int_{s_3-\epsilon_3}^{s_1+\epsilon_1} \frac{\exp\left\{-ut - ix\sqrt{\phi}\sqrt{\frac{(u-s_1)(s_2-u)}{s_3-u}}\right\}}{u} du. \tag{A.7}$$

Along HJ, the point $-s_1$ is moved to the origin by writing $s = \epsilon_1 e^{i\theta} - s_1$, $ds = i\epsilon_1 e^{i\theta} d\theta$. Thus

$$\begin{aligned}
&\frac{1}{2\pi i}\int_{HJ} e^{st} f(s) ds \\
&= \frac{\epsilon_1}{2\pi}\int_{\pi}^{-\pi} \frac{\exp\left\{\left(\epsilon_1 e^{i\theta} - s_1\right) t - x\sqrt{\phi}\sqrt{\epsilon_1} e^{i\theta/2}\sqrt{\frac{\epsilon_1 e^{i\theta} - s_1 + s_2}{\epsilon_1 e^{i\theta} - s_1 + s_3}} + i\theta\right\}}{\epsilon_1 e^{i\theta} - s_1} d\theta \\
&\to 0 \quad \text{as} \quad \epsilon_1 \to 0.
\end{aligned} \tag{A.8}$$

Along JK, let $s = u\, e^{i\theta}$, $\theta = -\pi$, $s + s_1 = u_1\, e^{i\theta_1}$, $\theta_1 = -\pi$, $s + s_2 = u_2\, e^{i\theta_2}$, $\theta_2 = 0$, $s + s_3 = u_3\, e^{i\theta_3}$, $\theta_3 = 0$, from $s = -s_1 - \epsilon_1$ to $s = -s_3 + \epsilon_3$:

$$\begin{aligned}
&\frac{1}{2\pi i}\int_{JK} e^{st} f(s) ds \\
&= \frac{1}{2\pi i}\int_{-s_1-\epsilon_1}^{-s_3+\epsilon_3} e^{st} f(s) ds \\
&= \frac{1}{2\pi i}\int_{s_1+\epsilon_1}^{s_3-\epsilon_3} \frac{\exp\left\{-ut + ix\sqrt{\phi}\sqrt{\frac{(u-s_1)(s_2-u)}{s_3-u}}\right\}}{u} du.
\end{aligned} \tag{A.9}$$

Along KL, the point $-s_3$ is moved to the origin by writing $s = \epsilon_3 e^{i\theta} - s_3$, $ds = i\epsilon_3 e^{i\theta} d\theta$. Thus,

$$\begin{aligned}
&\frac{1}{2\pi i}\int_{KL} e^{st} f(s) ds \\
&= \frac{\epsilon_3}{2\pi}\int_{0}^{-\pi} \frac{\exp\left\{ -x\sqrt{\frac{\phi}{\epsilon_3}} e^{-i\theta/2}\sqrt{\left(\epsilon_3 e^{i\theta} + s_1 - s_3\right)\left(\epsilon_3 e^{i\theta} - s_3 + s_2\right)} + i\theta \right\}}{\epsilon_3 e^{i\theta} - s_3} d\theta \\
&\to 0 \quad \text{as} \quad \epsilon_3 \to 0.
\end{aligned} \tag{A.10}$$

Along LM, let $s = u\, e^{i\theta}$, $\theta = -\pi$, $s + s_1 = u_1\, e^{i\theta_1}$, $\theta_1 = -\pi$, $s + s_2 = u_2\, e^{i\theta_2}$, $\theta_2 = 0$, $s + s_3 = u_3\, e^{i\theta_3}$, $\theta_3 = -\pi$, from $s = -s_3 - \epsilon_3$ to $s = -s_2 + \epsilon_2$:

$$\begin{aligned}
&\frac{1}{2\pi i}\int_{LM} e^{st} f(s) ds \\
&= \frac{1}{2\pi i}\int_{-s_3-\epsilon_3}^{-s_2+\epsilon_2} e^{st} f(s) ds \\
&= \frac{1}{2\pi i}\int_{s_3+\epsilon_3}^{s_2-\epsilon_2} \frac{\exp\left\{-ut - x\sqrt{\phi}\sqrt{\frac{(u-s_1)(s_2-u)}{u-s_3}}\right\}}{u} du.
\end{aligned} \tag{A.11}$$

Along MN, the point $-s_2$ is moved to the origin by writing $s = \epsilon_2 e^{i\theta} - s_2$, $ds = i\epsilon_2 e^{i\theta} d\theta$. Thus

$$\begin{aligned}
&\frac{1}{2\pi i}\int_{MN} e^{st} f(s)ds \\
&= \frac{\epsilon_2}{2\pi}\int_0^{-\pi} \frac{\exp\left\{\left(\epsilon_2 e^{i\theta} - s_2\right)t - x\sqrt{\phi}\sqrt{\epsilon_2}e^{i\theta/2}\sqrt{\frac{\epsilon_2 e^{i\theta}+s_1-s_2}{\epsilon_2 e^{i\theta}-s_2+s_3}} + i\theta\right\}}{\epsilon_2 e^{i\theta} - s_2}\, d\theta \\
&\to 0 \quad \text{as} \quad \epsilon_2 \to 0. \qquad \text{(A.12)}
\end{aligned}$$

Along NO, let $s = u\, e^{i\theta}$, $\theta = -\pi$, $s + s_1 = u_1\, e^{i\theta_1}$, $\theta_1 = -\pi$, $s + s_2 = u_2\, e^{i\theta_2}$, $\theta_2 = -\pi$, $s + s_3 = u_3\, e^{i\theta_3}$, $\theta_3 = -\pi$, from $s = -s_2 - \epsilon_2$ to $s = -R$:

$$\begin{aligned}
&\frac{1}{2\pi i}\int_{NO} e^{st} f(s)ds \\
&= \frac{1}{2\pi i}\int_{-s_2-\epsilon_2}^{-R} e^{st} f(s)ds \\
&= \frac{1}{2\pi i}\int_{s_2+\epsilon_2}^{R} \frac{\exp\left\{-ut + ix\sqrt{\phi}\sqrt{\frac{(u-s_1)(u-s_2)}{u-s_3}}\right\}}{u} du. \qquad \text{(A.13)}
\end{aligned}$$

Now, the residue at the simple pole $s = 0$ is

$$\lim_{s\to 0} \frac{s\exp\left\{st - x\sqrt{\phi}\sqrt{\frac{(s+s_1)(s+s_2)}{s+s_3}}\right\}}{s} = \exp\left\{-x\sqrt{\frac{\phi s_1 s_2}{s_3}}\right\}. \qquad \text{(A.14)}$$

By the residue theorem,

$$\frac{1}{2\pi i}\oint_C e^{st} f(s)ds = \exp\left\{-x\sqrt{\frac{\phi s_1 s_2}{s_3}}\right\}. \qquad \text{(A.15)}$$

Hence, with the integrals along BC, DE, FG, HJ, KL, MN, and OA tending to zero in the limit, and with the integrals along EF and LM cancelling through addition, the only contributions are those from the integrals along CD, GH, JK, and NO. Thus, (A.2) reduces to

$$\begin{aligned}
&\frac{1}{2\pi i}\int_{AB} e^{st} f(s)ds \\
&= \exp\left\{-x\sqrt{\frac{\phi s_1 s_2}{s_3}}\right\} \\
&\quad -\frac{1}{2\pi i}\lim_{R\to\infty,\epsilon_{1,2,3}\to 0}\left\{\begin{array}{c} \int_{CD} e^{st} f(s)ds + \int_{GH} e^{st} f(s)ds \\ + \int_{JK} e^{st} f(s)ds + \int_{NO} e^{st} f(s)ds \end{array}\right\} \\
&= \exp\left\{-x\sqrt{\frac{\phi s_1 s_2}{s_3}}\right\} \\
&\quad -\frac{1}{\pi}\left\{\begin{array}{c} \int_{s_2}^{\infty} \frac{e^{-ut}}{u}\sin\left(x\sqrt{\phi}\sqrt{\frac{(u-s_1)(u-s_2)}{u-s_3}}\right)du \\ + \int_{s_1}^{s_3} \frac{e^{-ut}}{u}\sin\left(x\sqrt{\phi}\sqrt{\frac{(u-s_1)(s_2-u)}{s_3-u}}\right)du \end{array}\right\}. \qquad \text{(A.16)}
\end{aligned}$$

The solutions for c_1 and c_2 follow directly from (A.16) using convolution.

Acknowledgments. We would like to thank the reviewers for their careful reading of the manuscript and for their suggestions and advice.

REFERENCES

[1] J. P. Abraham, J. M. Gorman, E. M. Sparrow, J. R. Stark, and R. E. Kohler, *A mass transfer model of temporal drug deposition in artery walls*, Int. J. Heat Mass Trans., 58 (2013), pp. 632–638.

[2] B. Balakrishnan, J. F. Dooley, G. Kopia, and E. R. Edelman, *Intravascular drug release kinetics dictate arterial drug deposition, retention, and distribution*, J. Controlled Release, 123 (2007), pp. 100–108.

[3] A. L. Baldwin, L. M. Wilson, I. Gradus-Pizlo, R. Wilensky, and K. March, *Effect of atherosclerosis on transmural convection and arterial ultrastructure*, Arterio. Thromb. Vasc. Biol., 17 (1997), pp. 3365–3375.

[4] K. M. Balss, G. Llanos, G. Papandreou, and C. A. Matyanoff, *Quantitative spatial distribution of sirolimus and polymers in drug-eluting stents using confocal Raman microscopy*, J. Biomed. Mater. Res. Part A, 85A (2007), pp. 258–270.

[5] B. E. Bierer, P. S. Patilla, R. F. Standaert, L. A. Herzenberg, S. J. Burakoff, G. Crabtree, and S. Schreiber, *Two distinct signal transmission pathways in T lymphocytes are inhibited by complexes formed between an immunophilin and either FK*506 *or rapamycin*, Proc. Natl. Acad., Sci. USA, 87 (1990), pp. 9231–9235.

[6] P. Biscari, S Minisini, D. Pierotti, G. Verzini, and P. Zunino, *Controlled release with finite dissolution rate*, SIAM J. Appl. Math., 71 (2011), pp. 731–752.

[7] A. Borghi, E. Foa, R. Balossino, F. Migliavacca, and G. Dubini, *Modelling drug elution from stents: Effects of reversible binding in the vascular wall and degradable polymeric matrix*, Comput. Methods Biomech. Biomed. Eng., 11 (2008), pp. 367–377.

[8] T. Casalini, M. Masi, and G. Perale, *Drug eluting sutures: A model for in vivo estimations*, Int. J. Pharm., 429 (2012), pp. 148–157.

[9] D. S. Cohen and T. Erneux, *Controlled drug release asymptotics*, SIAM J. Appl. Math., 58 (1998), pp. 1193–1204.

[10] S. Constantini, F. Maceri, and G. Vairo, *Un modelo del rilascio di farmaco in stent coronarici*, in Proceedings of the XVII National Congress of Computational Mechanics (GIMC), Alghero, Italy, 2008.

[11] S. Cook and S. Windecker, *Coronary artery stenting*, in Cardiovascular Catheterization and Intervention: A Textbook of Coronary, Peripheral, and Structural Heart Disease, CRC Press, Boca Raton, FL, 2010, pp. 412–428.

[12] J. Crank, *The Mathematics of Diffusion*, Clarendon Press Oxford, 1975.

[13] C. D'Angelo, P. Zunino, A. Porpora, S. Morlacchi, and F. Migliavacca, *Model reduction strategies enable computational analysis of controlled drug release from cardiovascular stents*, SIAM J. Appl. Math., 71 (2011), pp. 2312–2333.

[14] M. C. Delfour, A. Garon, and V. Longo, *Modeling and design of coated stents to optimize the effect of the dose*, SIAM J. Appl. Math., 65 (2005), pp. 858–881.

[15] L. Formaggia, S. Minisini, and P. Zunino, *Modeling polymeric controlled drug release and transport phenomena in the arterial tissue*, Math. Model. Methods Appl. Sci., 20 (2010), pp. 1759–1786.

[16] M. Grassi, G. Pontrelli, L. Teresi, G. Grassi, L. Comel, A. Ferluga, and L. Galasso, *Novel design of drug delivery in stented arteries: A numerical comparative study*, Math. Biosci. Eng., 6 (2009), pp. 493–508.

[17] T. Higuchi, *Rate of release of medicaments from ointment bases containing drugs in suspension*, J. Pharm. Sci., 50 (1961), pp. 874–875.

[18] M. Horner, S. Joshi, V. Dhruva, S. Sett, and S. F. C. Stewart, *A two-species drug delivery model is required to predict deposition from drug-eluting stents*, Cardiovasc. Eng. Technol., 1 (2010), pp. 225–234.

[19] D. R. Hose, A. J. Narracott, B. Griffiths, S. Mahmood, J. Gunn, D. Sweeney, and P. V. Lawford, *A thermal analogy for modeling drug elution from cardiovascular stents*, Comput. Methods Biomech. Biomed. Eng., 7 (2004), pp. 257–264.

[20] C. W. Hwang, D. Wu, and E. R. Edelman, *Physiological transport forces govern drug distribution for stent based delivery*, Circulation, 104 (2001), pp. 600–605.

[21] G. Karner and K. Perktold, *Effect of endothelial injury and increased blood pressure on albumen accumulation in the arterial wall: A numerical study*, J. Biomechs., 33 (2000), pp. 709–715.
[22] W. Khan, S. Farah, and A. J. Domb, *Drug eluting stents: Developments and current status*, J. Controlled Release, 161 (2012), pp. 703–712.
[23] V. B. Kolachalama, A. R. Tzafriri, D. Y. Arifin, and E. R. Edelman, *Luminal flow patterns dictate arterial drug deposition in stent-based delivery*, J. Controlled Release, 133 (2009) pp. 24–30.
[24] V. B. Kolachalama, E. G. Levine, and E. R. Edelman, *Luminal flow amplifies stent-based drug-deposition in arterial bifurcations*, PLoS ONE, 4 (2009), pp. 1–9.
[25] P. Libby, *Atherosclerosis: The New View*, Sci. Amer., 286 (2007), pp. 29–37.
[26] A. D. Levin, M. Jonas, C.-W. Hwang, and E. R. Edelman, *Local and systemic drug competition in drug-eluting stent tissue deposition properties*, J. Controlled Release, 109 (2005), pp. 236–243.
[27] D. Lloyde-Jones et al., *Heart disease and stroke statistics—*2010 *update: A report from the American Heart Association*, Circulation, 121 (2010), pp. e46–e215.
[28] M. A. Lovich and E. R. Edelman, *Computational simulations of local vascular heparin deposition and distribution*, Am. J. Physiol. Heart Circ. Physiol., 271 (1996), pp. H2014–H2024.
[29] A. Lusis, *Atherosclerosis*, Nature, 407 (2000), pp. 233–241.
[30] S. McGinty, S. McKee, R. M. Wadsworth, and C. McCormick, *Modelling drug-eluting stents*, Math. Med. Biol., 28 (2011), pp. 1–29.
[31] R. Mongrain, I. Faik, R. L. Leask, J. Rodes-Cabau, E. Larose, and O. F. Bertrand, *Effects of diffusion coefficients and struts apposition using numerical simulations for drug eluting coronary stents*, J. Biomech. Eng., 129 (2007), pp. 733–742.
[32] C. Murray and A. Lopez, *Alternative projections of mortality and disability by cause* 1990–2020: *Global burder of disease study*, The Lancet, 349 (1997), pp. 1498–1504.
[33] G. Pontrelli and F. de Monte, *Mass diffusion through two-layer porous media: An application to the drug eluting stent*, Int. J. Heat Mass Trans., 50 (2007), pp. 3658–3669.
[34] G. Pontrelli and F. de Monte, *Modelling of mass dynamics in arterial drug-eluting stents*, J. Porous Media, 12 (2009), pp. 19–28.
[35] G. Pontrelli and F. de Monte, *A multi-layer porous wall model for coronary drug-eluting stents*, Int. J. Heat Mass Trans., 53 (2010), pp. 3629–3637.
[36] S. Prabhu and S. Hossainy, *Modeling of degradation and drug release from a biodegradable stent coating*, J. Biomed. Mater. Res. Part A, 80A (2007), pp. 732–741.
[37] F. Rossi, T. Casalini, E. Raffa, M. Masi, and G. Perale, *Bioresorbable polymer coated drug eluting stent: A model study*, Mol. Pharm., 9 (2012), pp. 1898–1910.
[38] R. S. Schwartz, E. Edelman, R. Virmani, A. Carter, J. F. Granada, G. L. Kaluza, N. A. F. Chronos, K. A. Robinson, R. Waksman, J. Weinberger, G. J. Wilson, and R. L. Wilensky, *Drug-eluting stents in preclinical studies. Updated consensus recommendations for preclinical evaluation*, Circulation Cardiovascular Interventions, 1 (2008), pp. 143–1153.
[39] A. Seidlitz, S. Nagel, B. Semmling, N. Grabow, H. Martin, V. Senz, C. Harder, K. Sternberg, K.-P. Schmitz, H. K. Kroemer, and W. Weitschies, *Examination of drug release and distribution from drug-eluting stents with a vessel-simulating flow-through cell*, Eur. J. Pharm. Biopharm., 78 (2011), pp. 36–48.
[40] J. Siepmann, K. Elkharraz, F. Siepmann, and D. Klose, *How autocatalysis accelerates drug release from PLGA-based microparticles: A quantitative treatment*, Biomacromolecules, 6 (2005), pp. 2312–2319.
[41] J. Tambača, M. Kosor, S. Čanić, and D. Paniagua, *Mathematical modeling of vascular stents*, SIAM J. Appl. Math., 70 (2010), pp. 1922–1952.
[42] A. R. Tzafriri, A. Groothuis, G. Sylvester Price, and E. R. Edelman, *Stent elution rate determines drug deposition and receptor-mediated effects*, J. Controlled Release, 161 (2012), pp. 918–926.
[43] G. Vairo, M. Cioffi, R. Cottone, G. Dubini, and F. Migliavacca, *Drug release from coronary eluting stents: A multidomain approach*, J. Biomech., 43 (2010), pp. 1580–1589.
[44] C. Yang and H. M. Burt, *Drug-eluting stents: Factors governing local pharmacokinetics*, Adv. Drug Delivery Rev., 58 (2006), pp. 402–411.
[45] H. Q. Zhao, D. Jayasinghe, S. Hossainy, and L. B. Schwartz, *A theoretical model to characterize the drug release behavior of drug-eluting stents with durable polymer matrix coating*, J. Biomed. Mater. Res. Part A, 100A (2012), pp. 120–124.

[46] W. Zhu, T. Masaki, A. K. Cheung, and S. E. Kern, *In-vitro release of rapamycin from a thermosensitive polymer for the inhibition of vascular smooth muscle cell proliferation*, J. Bioequiv. Availab., 1 (2009), pp. 3–12.

[47] P. Zunino, *Multidimensional pharmacokinetic models applied to the design of drug-eluting stents*, Cardiov. Eng. Int. J., 4 (2004), pp. 181–191.

[48] P. Zunino, C. D'Angelo, L. Petrini, C. Vergara, C. Capelli, and F. Migliavacca, *Numerical simulation of drug eluting coronary stents: Mechanics, fluid dynamics and drug release*, Comput. Methods Appl. Mech. Engrg., 198 (2009), pp. 3633–3644.